Journal of Statistical Physics, Vol. 79, Nos. 1/2, 1995

Nearly Separable Behavior of Fermi–Pasta–Ulam Chains Through the Stochasticity Threshold

Carlo Alabiso,[1,2] Mario Casartelli,[1,3] and Paolo Marenzoni[4]

Received July 18, 1994; final October 13, 1994

For the periodic Fermi–Pasta–Ulam chain with quartic potential we prove the relation $\langle p_k^2 \rangle_T \approx (1+\alpha)\langle \omega_k^2 q_k^2 \rangle_T$, i.e., the proportionality, already at early times T, between averaged kinetic and harmonic energies of each mode. The factor α depends on the parameters of the model, but not on the mode and the number of degrees of freedom. It grows with the anharmonic strength from the value $\alpha = 0$ of the harmonic limit (virial theorem) up to few units for the system much above the threshold. In the stochastic regime the time necessary to reduce the fluctuations in k to a fixed percentage remains at least one order of magnitude smaller than the time necessary to reach a similar level of equipartition. The persistence of such a behavior even above the stochasticity threshold clarifies a number of previous numerical results on the relaxation to equilibrium: e.g., the existence of several time scales and the relevance of the harmonic frequency spectrum. The difficulties in the numerical simulation of the thermodynamic limit are also discussed.

KEY WORDS: Virial theorem; approach to equilibrium; Fermi–Pasta–Ulam model; stochasticity threshold; rates of energy exchanges; thermodynamic limit.

1. INTRODUCTION

From the very beginning of numerical simulations, anharmonic chains of oscillators have been among the most widely studied dynamical systems.[1,2] Such an interest was mainly driven by the KAM theory, more precisely, by

[1] Dipartimento di Fisica dell'Università di Parma, Parma, Italy. E-mail: alabiso@vaxpr.pr.infin.it.
[2] INFN, Sezione staccata di Parma, Parma, Italy.
[3] CNR-INFM.
[4] Dipartimento di Ingegneria dell'Informazione dell'Università di Parma, Parma, Italy.

0022-4715/95/0400-0451$07.50/0

the purpose of recognizing the transition from quasi-integrability to stochasticity in a physically significant range of the parameters. In a sense, the behavior above the stochasticity threshold has been overlooked, since this regime of motion was supposed to match the standard expectations of classical statistical mechanics.

To be definite, by stochasticity threshold we mean the transition between a low-anharmonicity regime, where the memory of the initial conditions influences the time averages forever, and a highly stochastic regime, where the equipartition theorem may be verified at any desired level of accuracy within a finite time.

However, nonlinear chains, even when stochastic, are not purely random systems, e.g., in the sense of the Boltzmann gas of hard spheres, and their approach to equilibrium presents a wide variety of behaviors. As discussed in a recent paper,[3] in some cases the symmetries of the Hamiltonian may be relevant for this phenomenology, in particular for the numerical experiments on the thermodynamic limit. These experiments have shown that the simulation of the limit fails when symmetries are present, since they introduce an anomalous behavior for the dynamical quantities near the conserved ones, which have been called *quasiconserved.* In order to get the thermalization via numerical calculations, the infinite time of the ergodic averages must be simulated, as usual, by a finite time, long, but constant all through the experiments. Actually, at increasing N, for groups of quasiconserved variables made up by *a fixed percentage* of the total modes, the time taken to reach the same level of thermalization essentially grows with N. This makes impossible the simulation of the thermodynamic limit.

We concentrate here on the one-dimensional Fermi–Pasta–Ulam (FPU) model[1,3] with quartic potential and periodic boundary conditions, as the best-known and most familiar model among those exhibiting the phenomenology described above. Furthermore, it presents another peculiarity which can be roughly described as the persistence, also above the stochasticity threshold, of a typical feature of the separable harmonic chains, as expressed by the virial theorem: precisely, the proportionality of the time-averaged kinetic and harmonic potential energies, for all modes and for early times. The proportionality factor does not depend on the mode and on the number of degrees of freedom, but it does depend on the parameters of the model: the specific energy and the relative strength of the harmonic and anharmonic potentials. It smoothly grows from the value 1 of the harmonic case (virial theorem) up to the few units of the whole model with the parameters three orders of magnitude above the stochasticity threshold. In this domain, the independence from the mode is obtained within a reasonable accuracy much before reaching a similar level

of equipartition, in times at least one order of magnitude smaller, independent of the parameters.

In a sense, this marks an inversion of the usual attitude: phenomena which do not feel the threshold, indeed, are expected to be practically chaotic even at low energies; we show on the contrary that even at high energies there persists a harmonic-like behavior for such meaningful observables as the normal modes.

We prove this property, a sort of *virial theorem*, in the appendix, since we prefer to present the results through a more phenomenological and intuitive approach, by introducing a specific ansatz of statistical nature, checked with numerical experiments.

These results explain why harmonic quantities and parameters, such as energies and spectrum, keep a relevant meaning also when anharmonicity cannot be considered a small perturbation. In particular, they explain a well-known characteristic of the FPU model, i.e., the reliability of equipartition of the harmonic energies as stochasticity criterion (which does not follow from the general equipartition theorem).

With a similar approach, even if not supported by analogous rigorous proof, we also derive the equipartition of the rates of variation of the action variables and the equivalent proportionality to the harmonic spectrum of the rates of energy exchanges,[3,4] which therefore go to zero for the low-frequency modes. This last property, in turn, is related to the greater rigidity of these modes in the approach to equilibrium.

Finally, we clarify the failure of the numerical simulation of the thermodynamic limit, specifying the role of various parameters in relation to the speed of thermalization of the modes. In this context, in order to check the reliability of the analysis, we introduce other (nonthermodynamic) limits, which allow us to get a prefixed value of suitable thermalization indicators *within a finite time independent of N*.

The paper is organized as follows: in Section 2 we recall generalities and main notations about nonlinear chains; in Section 3 we discuss the FPU model with some previous results, giving also the numerical specifications for the experimental tests; in Section 4 we propose and check the proportionality between kinetic and harmonic energies as a phenomenological ansatz; in Section 5 we introduce a similar ansatz relating the rates of variation of the action variables and the harmonic potential energies; the results of Section 5 are exploited in Section 6 to discuss the limit $N \to \infty$. Finally, in the appendix we provide an analytic estimate of the property introduced as an ansatz in Section 4.

2. THE HAMILTONIAN ANHARMONIC CHAINS

Let us start by recalling the main notations. The Lagrangian form of the harmonic term is

$$\mathscr{L}_0(\mathbf{x}) = K - \chi V_2 = \frac{1}{2}\sum_{i=1}^{N} \dot{x}_i^2 - \frac{\chi}{2}\sum_{i=1}^{N} (x_i - x_{i+1})^2 \qquad (x_1 \equiv x_{N+1}) \quad (1)$$

Through standard diagonalization $\mathbf{x} = \mathbf{Bq}$, where $\mathbf{B} = [\beta_{i,k}]$ is the unitary matrix

$$\beta_{i,k} = \left(\frac{2}{N}\right)^{1/2} C_k \cos\frac{2(k-1)i\pi}{N}, \qquad k = 1,..., M$$

$$\beta_{i,k} = \left(\frac{2}{N}\right)^{1/2} C_k \sin\frac{2(N-k+1)i\pi}{N}, \qquad k = M+1,..., N$$

with $M = [N/2] + 1$, $[N/2]$ being the integer part of $N/2$, and

$$C_k = \begin{cases} \dfrac{1}{\sqrt{2}}, & k = 1 \\ \dfrac{1}{\sqrt{2}}, & k = \dfrac{N}{2} + 1 \quad (N \text{ even}) \\ 1, & \text{otherwise} \end{cases}$$

the harmonic potential reads

$$\chi V_2 = \frac{\chi}{2}\sum_{i=1}^{N} (x_i - x_{i+1})^2 = \frac{1}{2}\sum_{k=1}^{N} \omega_k^2 q_k^2$$

and the corresponding Hamiltonian is

$$H_0(\mathbf{p}, \mathbf{q}) = \sum_{k=1}^{N} \tfrac{1}{2}(p_k^2 + \omega_k^2 q_k^2) = \sum_{k=1}^{N} E_k = \sum_{k=1}^{N} \omega_k J_k \qquad (2)$$

where E_k are the harmonic energies and J_k are the action variables; the harmonic spectrum is

$$\omega_k = 2\sqrt{\chi}\sin\frac{(k-1)\pi}{N} \qquad (3)$$

Consider now the anharmonic Hamiltonian $H = H_0 + V'$, with V' independent of the time t. The Hamiltonian equations, conserving the total energy E, read

$$\begin{aligned} \dot{q}_k(t) &= p_k(t) \\ \dot{p}_k(t) &= -\omega_k^2 q_k(t) - F_k(t) \end{aligned} \qquad (4)$$

where F_k denotes the anharmonic force on the kth mode:

$$F_k = -\frac{\partial V'}{\partial q_k} = -\sum_{i=1}^{N} \beta_{i,k} \frac{\partial V'}{\partial x_i} \tag{5}$$

Consider also the following observables:

$$\mathscr{Q}_k = \left\langle q_k \frac{\partial H}{\partial q_k} \right\rangle = \langle \omega_k^2 q_k^2 \rangle - \langle q_k F_k \rangle, \qquad \mathscr{P}_k = \left\langle p_k \frac{\partial H}{\partial p_k} \right\rangle = \langle p_k^2 \rangle \tag{6}$$

and

$$\mathscr{E}_k = \langle E_k \rangle \tag{7}$$

$$\mathscr{T}_k = \langle |\dot{J}_k| \rangle = \langle |\dot{E}_k| \rangle / \omega_k \tag{8}$$

where

$$\langle f(t) \rangle = \lim_{T \to \infty} \langle f(t) \rangle_T = \lim_{T \to \infty} \frac{1}{T} \int_0^T f(t)\, dt$$

denotes the time average. Since

$$\mathscr{Q}_k|_T \equiv \left\langle q_k \frac{\partial H}{\partial q_k} \right\rangle_T = -\frac{1}{T} \int_0^T q_k \dot{p}_k\, dt = \frac{1}{T} \int_0^T \dot{q}_k p_k\, dt - \frac{1}{T} [q_k p_k]_0^T$$

it follows that

$$\mathscr{P}_k|_T = \langle p_k^2 \rangle_T = \langle \omega_k^2 q_k^2 \rangle_T - \langle q_k F_k \rangle_T + O\left(\frac{1}{T}\right) = \mathscr{Q}_k|_T + O\left(\frac{1}{T}\right) \tag{9}$$

In the following, T always will be larger than the time necessary to make negligible the differences between $\mathscr{P}_k|_T$ and $\mathscr{Q}_k|_T$. In any case, $\mathscr{P}_k = \mathscr{Q}_k$. The term $-q_k\, \partial H/\partial q_k$ is known as the virial of Clausius of the kth mode; for harmonic chains ($F_k = 0$), formula (9) states one possible form of the virial theorem, i.e., the equality between time-averaged kinetic and potential energies *for each mode*.

Observables (6), via the standard equipartition theorem, are equal to each other in the stochastic regime of motion; moreover, it is experimentally known that also the mean harmonic energies $\mathscr{E}_k$ tend to a common value in many Hamiltonian systems (this is indeed a widely used criterion of stochasticity). As to the $\mathscr{T}_k$ observables, there is a large pattern of behavior distinguishing different models.[3–5] In ref. 3 it was shown that the onset of the asymptotic behavior for $\mathscr{P}_k$, $\mathscr{Q}_k$, $\mathscr{E}_k$, and $\mathscr{T}_k$ admits, at finite

times, large deviations which increase at growing N, as will be discussed more extensively in Section 6. These deviations are related to the existence of *quasi constants of motion.*

3. THE FERMI–PASTA–ULAM SYSTEM

The quartic FPU periodic system is characterized by the anharmonic potential

$$V' = \varepsilon V_4(\mathbf{x}) = \frac{\varepsilon}{4} \sum_{i=1}^{N} (x_i - x_{i+1})^4 \qquad (x_1 \equiv x_{N+1}) \tag{10}$$

Since V_4 is translationally invariant, as the harmonic system is, the first mode decouples, implying the conservation of E_1. The total momentum p_1 is also conserved because $\omega_1 = 0$.

The anharmonic forces read

$$\begin{aligned} F_k &= -\varepsilon \sum_{i=1}^{N} [(x_i - x_{i+1})^3 + (x_i - x_{i-1})^3] \beta_{i,k} \\ &= -\varepsilon \omega_k \sum_{i=1}^{N} (x_i - x_{i+1})^3 \gamma_{i,k} \end{aligned} \tag{11}$$

where the new matrix $[\gamma_{i,k}]$, defined as

$$\gamma_{i,k} = \begin{cases} 0, & k = 1 \\ (1/\omega_k)(\beta_{i,k} - \beta_{i+1,k}), & k = 2,\ldots, N \end{cases}$$

assumes the explicit form

$$\gamma_{i,k} = \frac{1}{\sqrt{\chi}} \left(\frac{2}{N}\right)^{1/2} C_k \begin{cases} \sin \dfrac{\pi(k-1)(2i+1)}{N}, & k = 1,\ldots, M \\ -\cos \dfrac{\pi(N-k+1)(2i+1)}{N}, & k = M+1,\ldots, N \end{cases} \tag{12}$$

The matrix $[\gamma_{i,k}]$ satisfies

$$(x_i - x_{i+1}) = \sum_{j=2}^{N} \gamma_{i,j} \tilde{q}_j, \qquad \chi \sum_{i=1}^{N} (x_i - x_{i+1}) \gamma_{i,k} = \tilde{q}_k \tag{13}$$

where we used the variable $\tilde{q}_k$, homogeneous to p_k, defined as

$$\tilde{q}_k = \omega_k q_k \tag{14}$$

The following orthogonality conditions hold:

$$\sum_{i=1}^{N} \gamma_{i,j}\gamma_{i,k} = \frac{1}{\chi}\delta_{jk} \qquad (j,k=2,\ldots,N) \tag{15}$$

The numerical simulations quoted in the following have been performed on a VAX 4090 at low N and on a Connection Machine CM2 (both at the University of Parma) at high N. The equations of motion have been integrated through a standard fifth-order Runge-Kutta routine, using double precision (64 bits), mostly with a step $\Delta t = 0.005$. All this ensures a conservation of the energy within $1/10^5$ in the worst case, which is much better than the one usually accepted in this field, but it is necessary for some specific calculations. The time averages pick up one value every 100 steps, after a transient of 80,000 steps. Total times reach 10,000,000 steps. With $\chi = 1$, this corresponds approximately to 16,000 minimal harmonic periods (these are independent of N, whereas the longest periods diverge with N).

Once the specific energy $u = E/N$ is fixed, initial conditions are chosen randomly in the positions and velocities. Several choices in this class have been tested, with results qualitatively stable, as expected, apart from details for the lateral modes, i.e., for low frequencies. Of course, below threshold all the modes must be excited.

The main results of ref. 3 can be illustrated with the help of Fig. 1. It shows the variables $\mathscr{P}_k|_T = \langle p_k^2 \rangle_T$ for $k = 2,\ldots, 512$, $\chi = 1$, $\varepsilon = 0.1$, and $u = 10$. These values ensure we are above the stochasticity threshold. The time T is clearly insufficient for a good equipartition, which would be reached at any desired level just waiting longer. As Fig. 1 suggests, the modes get equipartitioned at different speeds: faster for the central modes and slower for the lateral ones. Moreover, whereas the speed of thermalization of the central modes remains constant, the speed of the lateral modes becomes slower and slower as N increases. This means that the "computational" thermodynamic limit $N \to \infty$ cannot be performed, as usual, at fixed time T, no matter how large it will be chosen.

This can be understood by observing that in (11) the factorization of the harmonic frequency ω_k is not a trivial one [see (12)]. Consequently, the anharmonic force has in front a factor $\sin[(k-1)\pi/N]$, which is $\ll 1$ for the lateral modes, i.e., for k near 2 or near N, while it is $O(1)$ for the central modes. Provided that the dependence on k of the other factor in (11) does not modify significantly such behavior, this identifies the lateral modes as *quasiconserved quantities*. From here, the greater rigidity of the lateral modes follows. In ref. 3 we stressed the "sinus-like" shape of $\langle |\dot{E}_k| \rangle$, which are the variables connected to the activity of the modes (see Fig. 4 below).

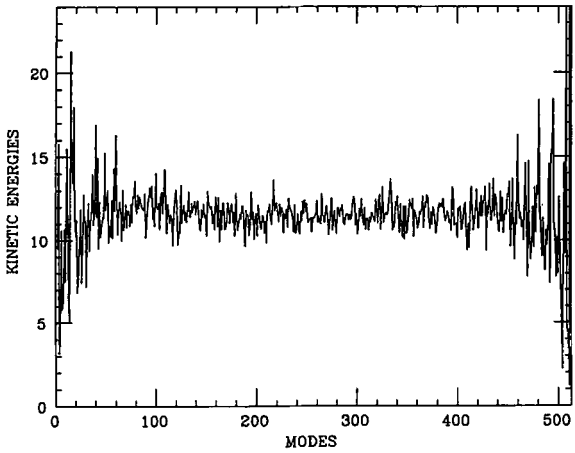

Fig. 1. Time-averaged kinetic energy $\langle p_k^2 \rangle_T$. Parameters: $N=512$, $\chi=1$, $\varepsilon=0.1$, $u=10$. Time step $\Delta t=0.005$, total time $T=400{,}000 \cdot \Delta t$, sample of 4000 averaged instantaneous values.

Independently, the approach leading to formula (11) has been suggested in ref. 6 for the FPU model using an equivalent transformation. Moreover, Ruffo[7] noticed that (11) (or equivalent formulas) qualitatively explains our previous phenomenology for all the models studied in ref. 3.

A more complete treatement of this point will be developed in the Sections 5 and 6.

4. THE VIRIAL OF CLAUSIUS IN THE FPU CHAIN

We discuss now another interesting peculiarity of the FPU model, found in that context but not previously discussed: at a value T longer than the time necessary to make $\mathscr{P}_k|_T = \mathscr{Q}_k|_T$ as suggested in (9), $\mathscr{P}_k|_T$ is also indistinguishable, if properly scaled, from $\mathscr{E}_k|_T$. They result to be proportional to each other, and clearly both to $\langle \tilde{q}_k^2 \rangle_T$, *much before* reaching a similar level of equipartition. This fact is illustrated in Fig. 2, which represents the ratio $\mathscr{P}_k|_T / \langle \tilde{q}_k^2 \rangle_T$, i.e., the same variable of Fig. 1, normalized at $\langle \tilde{q}_k^2 \rangle_T$. Note that the scales of the two figures are proportional to their mean values, so that the comparison between them gives a proper feeling for proportionality versus equipartition. This phenomenon has nothing to do with the stochasticity of the motion (apart from exceptional initial conditions below threshold); in fact, it takes place also for low values of u, or equivalently for low values of ε down to the harmonic value $\varepsilon=0$. By varying the parameters, the proportionality factor smoothly grows from

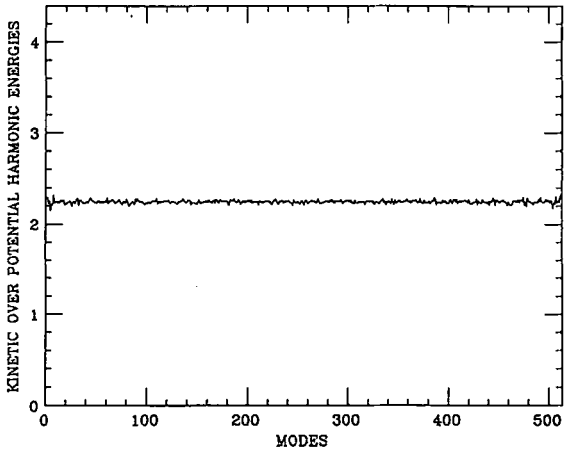

Fig. 2. Ratio between time-averaged kinetic and potential harmonic energies $\langle p_k^2 \rangle_T / \langle \tilde{q}_k^2 \rangle_T$. Same parameters as in Fig. 1.

the value 1 required by the virial theorem for $\varepsilon = 0$ [see (9)], up to the value readable in Fig. 2. [As for the time, see after (21)].

The proportionality we are speaking about will be proven in the appendix, giving rise to a sort of virial theorem specific for this model. However, for a better understanding, we present an argument which is very useful for the intuitive treatment of the virial terms, particularly with regard to the role of the parameters.

We begin by studying the anharmonic virial:

$$-\langle q_k F_k \rangle_T = \varepsilon \left\langle \sum_{i=1}^{N} (x_i - x_{i+1})^3 \gamma_{i,k} \tilde{q}_k \right\rangle_T \tag{16}$$

which, via formula (9), connects $\mathscr{P}_k|_T$ and $\langle \tilde{q}_k^2 \rangle|_T$. Formula (9) and the comparison between Figs. 1 and 2 lead to the ansatz

$$-\langle q_k F_k \rangle_T \approx \alpha_T \langle \tilde{q}_k^2 \rangle_T \tag{17}$$

with $\alpha_T \approx 1.25$ independent of k. The value $\alpha_T + 1$ can be read directly in Fig. 2. The convergence to the time-independent value $\alpha \approx 1.22$ is very fast.

To figure out the dependence of α_T on the parameters, consider the identity

$$\begin{aligned} -\langle q_k F_k \rangle_T &= \varepsilon \sum_{i=1}^{N} \gamma_{i,k} \langle (x_i - x_{i+1})^2 (x_i - x_{i+1}) \tilde{q}_k \rangle_T \\ &= \varepsilon \sum_{i=1}^{N} \gamma_{i,k} \eta_{ikT} \langle (x_i - x_{i+1})^2 \rangle_T \langle (x_i - x_{i+1}) \tilde{q}_k \rangle_T . \end{aligned} \tag{18}$$

which simply represents the definition of the correlation η_{ikT} among the two terms in the time average, i.e., $(x_i - x_{i+1})^2$ and $(x_i - x_{i+1})\tilde{q}_k$.

Because of the $i \to i+1$ shift invariance of the Hamiltonian and the chaoticity of the x_i variables (in practice, also below threshold), the time averages are expected to converge very rapidly to a value independent of the index i, leading to

$$\langle (x_i - x_{i+1})^2 \rangle_T \approx \left\langle \frac{2V_2}{N} \right\rangle_T$$

(This can be easily tested.) Therefore this factor can be extracted out of the sum (18):

$$-\langle q_k F_k \rangle_T \approx \varepsilon \left\langle \frac{2V_2}{N} \right\rangle_T \sum_{i=1}^{N} \gamma_{i,k} \eta_{ikT} \langle (x_i - x_{i+1})\tilde{q}_k \rangle_T \tag{19}$$

From (19), taking into account (13), a possible realization of the ansatz (17) is given by $\eta_{ikT} \approx A$ independent of i, k, and T. Therefore

$$\alpha_T = \tilde{\varepsilon} A \left\langle \frac{2V_2}{N} \right\rangle_T, \qquad \tilde{\varepsilon} = \varepsilon/\chi \tag{20}$$

Actually, the weak dependence of η_{ikT} on i, k, and T is quite reasonable: on i, once again, because of the shift invariance and the chaoticity of the $(x_i - x_{i+1})^2$ terms; on k since there exists only the relation (13) between the N variables $(x_i - x_{i+1})$ and the single kth mode; on T because of the fast stabilization of the time averages of the powers of $(x_i - x_{i+1})$. Therefore, the quantity A substantially describes the correlation due to the factorization of $(x_i - x_{i+1})^3$. Since in this factorization the other parameters are not involved, A is assumed independent of them. [The analytical derivation of (20) in the appendix includes the quantitative estimate of A.]

The experiments at high N, as in Figs. 1 and 2, are particularly significant because of the relevant phenomena of deviations from equipartition recalled in Section 3. Actually, we performed also economical experiments at low N, notably $N = 33$, stressing the fact that formula (20) does not require necessarily high N.

At $N = 33$, $u = 10$, $\varepsilon = 0.1$, and $\chi = 1$, from (17) we obtain, for α_T at several times, the following computational results:

$$\begin{aligned} &\alpha_{T_1} \approx 1.30 \pm 5\%, \qquad \alpha_{T_2} \approx 1.24 \pm 4\% \\ &\alpha_{T_3} \approx 1.23 \pm 3\%, \qquad \alpha_{T_4} \approx 1.22 \pm 1\% \end{aligned} \tag{21}$$

The times T_1–T_4 correspond to 100,000, 400,000, 1,200,000, and 4,000,000 steps, and the deviations are far below the corresponding deviations in k of $\mathscr{P}_k|_T$. For example, at the times T_1 and T_3, the equipartition of the latter variables is very poor, especially for the low-frequency modes: $\mathscr{P}_k|_T$ still varies over two orders of magnitude at T_1, and by 50% at T_3. From (21), (20), and the independent evaluation of the early stabilized $\langle V_2/N\rangle_T$, the estimate

$$A \approx 2.4 \tag{22}$$

can be deduced. Analogous experiments at very low energy, e.g., $u = 0.001$, give $A \approx 2.9$ as a good approximation. Both values are independent of u in the two domains, and the correlation A undergoes a transition through the stochasticity threshold (see the appendix for an explanation of this fact), more precisely, between $u = 1$ and $u = 5$, when $\chi = 1$ and $\varepsilon = 0.1$.

The fast convergence in T of α_T and of $\langle V_2/N\rangle_T$ justifies in the following the omission of the subscript T for these quantities, much before the onset of a good equipartition. The physically significant estimates for the kinetic terms and for the harmonic energies now read

$$\langle p_k^2\rangle_T \approx (1+\alpha)\langle \tilde{q}_k^2\rangle_T, \qquad \langle E_k\rangle_T \approx \tfrac{1}{2}(2+\alpha)\langle \tilde{q}_k^2\rangle_T \tag{23}$$

As a final step, by considering the whole Hamiltonian we derive the complete dependence of α on the parameters, through the evaluation of the factor $\langle V_2/N\rangle$ contained in (20). In analogy with the treatment of the quadratic term $\langle (x_i - x_{i+1})^2\rangle_T$ in (18), the estimate for the time average of the anharmonic potential gives

$$\begin{aligned}\langle V_4\rangle_T &= \frac{1}{4}\left\langle \sum_{i=1}^{N} (x_i - x_{i+1})^4 \right\rangle_T \approx \frac{A}{4}\left\langle \frac{2V_2}{N}\right\rangle \left\langle \sum_{i=1}^{N} (x_i - x_{i+1})^2 \right\rangle_T \\ &= AN\left(\left\langle \frac{V_2}{N}\right\rangle\right)^2 \end{aligned} \tag{24}$$

Collecting (23) and (24), we find that the time average of the specific energy reads

$$\begin{aligned} u \equiv \frac{E}{N} &= \frac{1}{N}\left(\left\langle \sum_{k=1}^{N} E_k \right\rangle + \varepsilon\langle V_4\rangle\right) \\ &\approx \frac{1}{2N}(2+\alpha)\left\langle \sum_{k=1}^{N} \tilde{q}_k^2 \right\rangle + \varepsilon A\left(\left\langle \frac{V_2}{N}\right\rangle\right)^2 \end{aligned} \tag{25}$$

By using the explicit form of α and by introducing the unknown

$$y = \left\langle \frac{V_2}{N} \right\rangle$$

we find for Eq. (25)

$$3\tilde{\varepsilon}Ay^2 + 2y - u/\chi = 0 \Rightarrow y = \frac{(1 + 3A\tilde{\varepsilon}u/\chi)^{1/2} - 1}{3\tilde{\varepsilon}A} \tag{26}$$

Inserting the values $\chi = 1$, $\varepsilon = 0.1$, $u = 10$, and the estimate $A = 2.4$, we obtain

$$y = 2.59 \tag{27}$$

which is within 2% of the experimental value at T_4.

At greater N, for example, $N = 512$, all the numerical data given above are confirmed, so that we assume the explicit form

$$\alpha = \tfrac{2}{3}[(1 + 3A\tilde{\varepsilon}u/\chi)^{1/2} - 1] \tag{28}$$

above and below threshold, with the two different values for the correlation A mentioned before.

Formulas (17) and (28) have been successfully checked in the following ranges: $32 \leqslant N \leqslant 2048$, $0 \leqslant \varepsilon \leqslant 0.2$, $0.001 \leqslant u \leqslant 100$, and $\chi = 1, 2$, taking into account the transition of A through the threshold.

5. THE RATES OF VARIATION OF ENERGIES AND ACTION VARIABLES

Because of the physical meaning of the variables, in this section we restrict our analysis above threshold.

The same kind of proportionality between $\mathscr{P}_k|_T$ and $\langle \tilde{q}_k^2 \rangle_T$ illustrated in Fig. 2 also has been found between $\mathscr{T}_k|_T$ and $\langle \tilde{q}_k^2 \rangle_T$, even if not as sharp as the previous one. Therefore, in the same spirit of ansatz (17), we could write

$$\mathscr{T}_k|_T \approx \xi \langle \tilde{q}_k^2 \rangle_T$$

assuming this relation as an independent ansatz. We do not have a rigorous deduction of this, as done in the appendix for (17). However, it is possible to connect ξ with the parameters, as for α in Section 4, in order to obtain a form accessible to experimental checks.

Since $E_k = \frac{1}{2}(p_k^2 + \tilde{q}_k^2)$, by using the Hamilton equations, we have that

$$\dot{E}_k = p_k F_k, \qquad \dot{J}_k = \frac{p_k}{\omega_k} F_k$$

and

$$\mathscr{T}_k = \langle |\dot{J}_k| \rangle = \langle |\dot{E}_k| \rangle / \omega_k = \langle |(p_k/\omega_k) F_k| \rangle$$

In analogy with (19), substituting there $\tilde{q}_k$ with p_k, we obtain

$$\left\langle \left| \frac{p_k}{\omega_k} F_k \right| \right\rangle_T \approx \tilde{\varepsilon} A' \left\langle \frac{2V_2}{N} \right\rangle \langle |p_k \tilde{q}_k| \rangle_T = \frac{1}{2\omega_k} R\alpha \left\langle \left| \frac{d}{dt} \tilde{q}_k^2 \right| \right\rangle_T \tag{29}$$

with $R = A'/A$. This estimate is well satisfied with $A' \approx 3$, even if not as precisely as (28).

As for the right-hand side of (29), by definition,

$$\left\langle \left| \frac{d}{dt} \tilde{q}_k^2 \right| \right\rangle_T = \frac{1}{T} \int_0^T \left| \frac{d}{dt} \tilde{q}_k^2 \right| dt = \frac{2}{T} \int_0^T |\tilde{q}_k \dot{\tilde{q}}_k| \, dt \tag{30}$$

We divide the integration interval 0–T in correspondence with the zeros t_i^k of the function $\tilde{q}_k \dot{\tilde{q}}_k$. In each subinterval t_i^k–t_{i+i}^k the modulus can be eliminated by simply extracting a sign: then the integral of the derivative is the difference of $\tilde{q}_k^2$ at the ends of the subinterval, where either $\tilde{q}_k$ or $\dot{\tilde{q}}_k$ vanishes. Clearly, only the points where $\dot{\tilde{q}}_k$ vanishes give a nonzero contribution. On the other hand, between two zeros of a sufficiently regular function, there are $2m_i - 1$ zeros of the derivative, i.e., m_i relative maxima interlaced with $m_i - 1$ relative minima where the function is positive. The maxima and the minima contribute, and each one twice, with a plus and a minus sign, respectively. Therefore

$$\int_0^T \left| \frac{d}{dt} \tilde{q}_k^2 \right| dt = 2 \sum_{i=1}^{n_k} \left\{ \sum_{j=1}^{m_i - 1} [\tilde{q}_k^2(t_{i,2j-1}^k) - \tilde{q}_k^2(t_{i,2j}^k)] + \tilde{q}_k^2(t_{i,2m_i-1}^k) \right\} \tag{31}$$

where $t_{i,1}^k, t_{i,3}^k, \ldots$ are the points of relative maximum and $t_{i,2}^k, t_{i,4}^k, \ldots$ are the interlaced points of relative minimum of $\tilde{q}_k(t)$. Of course, where the function is negative, maxima–minima and plus–minus signs have to be interchanged.

To proceed further, we introduce some simplifying hypotheses on the time evolution of orbits which will be discussed later. If the motion of the modes, even in the stochastic region, is "sinus-like," i.e., sufficiently regular

to allow only one maximum (or one minimum) between two zeros, then in (31) the internal sum would reduce to one single term, leading to

$$\int_0^T \left| \frac{d}{dt} \tilde{q}_k^2 \right| dt = 2 \sum_{i=1}^{n_k} \tilde{q}_k^2(\tilde{t}_i^k) \tag{32}$$

with $(\tilde{t}_i^k)$ being the points of relatie maximum (or minimum) in each half-period. If further the motion is even more regular, oscillating with fixed frequency (and possibly modulated amplitude), then the time interval $\Delta t_i^k = t_{i+1}^k - t_i^k$ is a Δ^k independent of i. Therefore, the sum (32) multiplied by the time interval Δ^k represents the integral of $\tilde{q}_k^2(t)$, apart from an overestimate due to the evaluation of $\tilde{q}_k^2(t)$ only in the maxima. With an exactly sinusoidal behavior of $\tilde{q}_k(t)$ in each half-period such an overestimate is given by a factor 2, independent of the modulation in amplitude.

Under all these hypotheses on the motion, collecting (30) and (32), we obtain

$$\left\langle \left| \frac{d}{dt} \tilde{q}_k^2 \right| \right\rangle_T = 2 \frac{1}{T} \sum_{i=1}^{n_k} \tilde{q}_k^2(\tilde{t}_i^k) \approx \frac{4}{\Delta^k} \langle \tilde{q}_k^2 \rangle_T \tag{33}$$

where Δ^k is the assumed half-period of the mode k.

To check the assumptions above, we have explicitly explored the functions $q_k(t)$, observing that, differently than in the x_i picture, the stochastic regime of motion does not destroy a certain kind of regularity, in the following sense:

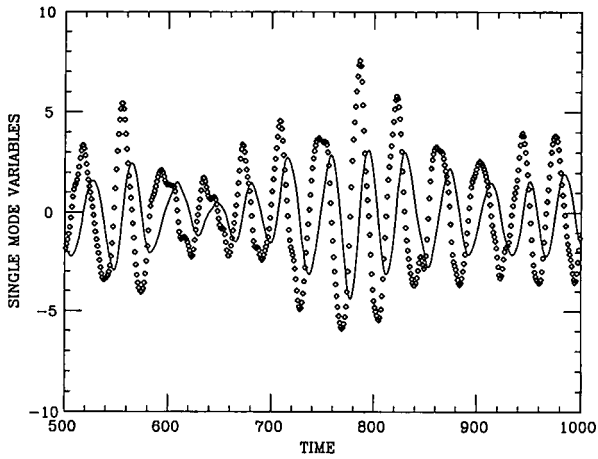

Fig. 3. Time behaviors of $q_k(t)$ (continuous line) and $p_k(t)$ (diamonds) for $k = 100$. Window of $10{,}000 \cdot \Delta t$ after a long transient, steps of $20 \cdot \Delta t$. Same parameters as in Fig. 1.

• There is an oscillating behavior with *almost equally spaced* zeros for $q_k(t)$ and *interlaced* zeros for $\dot{q}_k(t)$; this means that, even if the amplitudes are varying in time, it is possible to define an "effective period" $2\Delta^k$ (or an "effective frequency" $\tilde{\omega}_k$) (Fig. 3).

• Moreover, the ratio between the harmonic and the effective frequencies is independent of k within a few percent; it can be evaluated through direct inspection on plots as in Fig. 3 or, better, by numerical experiments on (33). This formula is very well satisfied and gives the proportionality factor between $\tilde{\omega}_k$ and ω_k independent of k within a few percent.

Therefore, the actual motion of normal modes in the anharmonic FPU system can be compared to the motion of "effective" harmonic oscillators with rescaled frequencies $\tilde{\omega}_k$ and modulated amplitudes, i.e., exactly the kind of motion considered for deriving formulas (32)–(33). As noticed before, these observations do not regard time averages, and they just require a reasonable transient time.

This phenomenology (partially known for a long time) is connected to the persistence of harmonic features in stochastic anharmonic systems. Precisely, consider again the anharmonic oscillators

$$\ddot{q}_k = -\omega_k^2 q_k - \varepsilon\omega_k \sum_{i=1}^{N} (x_i - x_{i+1})^3 \gamma_{i,k}$$

Inspired by the previous successful ansatz, in the cubic terms we extract the factors $(x_i - x_{i+1})^2$ as a noise (uniform in i) acting on linear forces, i.e.,

$$\ddot{q}_k \approx -\omega_k^2 q_k - \varepsilon\omega_k \alpha\chi \sum_{i=1}^{N} (x_i - x_{i+1})\gamma_{i,k} = -\omega_k^2(1+\alpha)q_k \tag{34}$$

Of course, this procedure is meaningless for instantaneous observations, but Eq. (34) is consistent with the behaviors described above (Fig. 3), apart from the modulation in amplitude, which may be attributed to the time dependence of the extracted factor. Actually, we use the same symbol α in (34) and in (20) for simplicity, because they turn out to be numerically identical [see below after (35)]. Equation (34) represents the motion of "effective" oscillators with frequencies $\tilde{\omega}_k$ and related half-periods Δ^k:

$$\tilde{\omega}_k = \omega_k(1+\alpha)^{1/2}, \qquad \Delta^k = \frac{\tilde{\tau}_k}{2} = \frac{\pi}{\tilde{\omega}_k} \tag{35}$$

The measure of Δ^k through (33), assuming the rescaling factor $(1+\alpha)^{1/2}$, gives for α the same numerical value as in (20). By collecting (29), (33), and (35), we finally obtain

$$\mathscr{T}_k|_T \approx R\alpha \frac{2(1+\alpha)^{1/2}}{\pi} \langle \tilde{q}_k^2 \rangle_T \approx 1.4 \langle \tilde{q}_k^2 \rangle_T \tag{36}$$

which is close to the experimental result within a few percent.

Formula (36) can also explain the typical pattern of Fig. 1, i.e., the differences between central and lateral modes. Indeed, (36) multiplied by ω_k gives the rates of energy exchange

$$\langle |\dot{E}_k| \rangle_T \approx \omega_k R\alpha \frac{2(1+\alpha)^{1/2}}{\pi} \langle \tilde{q}_k^2 \rangle_T \tag{37}$$

which measure the activities of the modes (roughly connected to the speed of thermalization).

The plot of these observables is reported in Fig. 4, which reproduces Fig. 9 of ref. 3 at earlier T and $N=512$ instead of 1024. It is noteworthy that possible large oscillations of $\langle \tilde{q}_k^2 \rangle_T$ are smoothed out by the vanishing of ω_k for k near 2 or N. The consequent vanishing of $\langle |\dot{E}_k| \rangle_T$ implies that the lateral modes have a much slower activity than the central ones, and that the connected observables have much slower variations. In other terms, whereas the initial data have no influence on the *global* pattern of

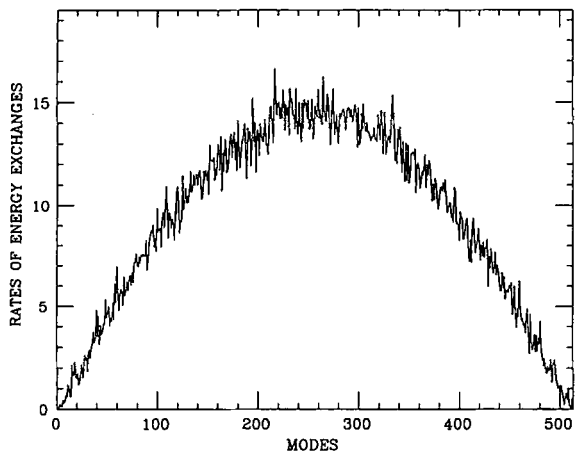

Fig. 4. Time-averaged absolute rates of energy exchange $\langle |\dot{E}_k| \rangle_T$. Same parameters as in Fig. 1.

Fig. 1, they do influence for a very long time the values of the *single* lateral modes. Formula (37) therefore explains the results presented in ref. 3 at fixed N.

To summarize the results of Sections 4 and 5, all our estimates (23), (24), (28), and (36) are essentially based on the ansatz (20) and its analogs (29) and (34). They depend on the constants A and A', testable experimentally once forever, above and below threshold as far as A is concerned, only above, as far as A' is concerned.

6. LARGE-N BEHAVIOR

The large-N behavior above threshold may be explored, either by keeping constant the parameters ε, χ, and u (i.e., in the thermodynamic limit) or by varying them with the purpose of controlling the relaxation times in the approaches to equilibrium.

As already observed in the introduction, the thermodynamic limit regards the limit $N \to \infty$ of time-averaged quantities over infinite time. From an experimental point of view, numerical tests require that we operate at growing N and "large" times: large, in the stochastic region, means at least the time T necessary to reach a pre-fixed sufficiently small level of equipartition. Such a time should be independent of N, in order to simulate the infinite-time average. We have shown in ref. 3 that this time T, on the contrary, increases with N, so that the experimental thermodynamic limit is not well defined. More precisely, along the indications of Fig. 1, we choose a fixed percent of central and lateral modes (e.g., 70% and 30%, respectively), observing at growing N the times necessary to reach a certain level of equipartition, defined by a given value of the variance of the observables (6) and (7). These times are roughly constant for the central modes, and grow with N for the lateral ones.

This can be better understood now within our estimates (37) for the time-averaged modulus of rates of energy exchange. In the thermodynamic limit, as follows from (28), α remains constant, as much as the average value of $\langle \tilde{q}_k^2 \rangle_T$, i.e., $2y$ [see (26)]. In other terms, Fig. 4 remains always similar to itself, i.e., $\langle |\dot{E}_k| \rangle_T \sim \omega_k$: the modes thicken in the whole spectrum, therefore around finite values (with a constant maximum) for high frequencies, around zero for low frequencies. In this limit, lateral modes have a slower and slower activity, explaining the experimental results quoted above.

As suggested by Fig. 4, fluctuations of $\langle \tilde{q}_k^2 \rangle_T$ occur in the whole spectrum, but they are irrelevant around the central modes (because the mean value is high) and have consequences only for details around low frequencies.

Instead of rates of energy exchange, one could equivalently consider the harmonicity-breaking force (clearly, time-averaged in modulus). Proceeding as in (29), we obtain the relation

$$\langle |F_k| \rangle_T \approx R\alpha\omega_k \langle |\tilde{q}_k| \rangle_T$$

which has been successfully checked.

Furthermore, we studied other (nonthermodynamic) limits, in order to explore the possibility of keeping the thermalization time bounded in the whole spectrum at growing N. On the basis of Eq. (37), this can be achieved by imposing, for example, that the number of "quasiharmonic modes" does not increase with N, or requiring that $\langle |\dot{E}_k| \rangle_T$ does not vanish in the limit. We can keep the specific volume $y = \langle V_2/N \rangle_T \sim \text{const}$, with the following conditions:

$$u \sim N^c, \qquad \varepsilon \sim N^c, \qquad \chi \sim N^c \tag{38}$$

Among these conditions, it is possible to choose c in such a way that the rates of energy exchange remain not decreasing. In a number of successful numerical experiments (also supporting the reliability of the ansatz) we chose $c = 1$, i.e., $u \sim N$, etc., which corresponds to keeping $\langle |\dot{E}_k| \rangle_T \propto \sqrt{N}$ for the lateral modes. With the limit (38), we found as expected a finite upper value for the equipartition time, given by the slower modes. As for the central modes, since $\langle |\dot{E}_k| \rangle_T \propto N\sqrt{N}$, their thermalization is even faster than in the usual thermodynamic limit.

APPENDIX. THE ESTIMATES

To derive analytically the ansatz (20), including the value of the parameter A, consider the identity

$$\begin{aligned} -q_k F_k &= \varepsilon \sum_{i=1}^{N} (x_i - x_{i+1})^3 \gamma_{i,k} \tilde{q}_k \\ &= \varepsilon \sum_{i=1}^{N} \{\gamma_{i,k}^4 \tilde{q}_k^4 + 3[(x_i - x_{i+1}) - \gamma_{i,k}\tilde{q}_k]^2 \gamma_{i,k}^2 \tilde{q}_k^2 \\ &\quad + 3[(x_i - x_{i+1}) - \gamma_{i,k}\tilde{q}_k]\gamma_{i,k}^3 \tilde{q}_k^3 \\ &\quad + [(x_i - x_{i+1}) - \gamma_{i,k}\tilde{q}_k]^3 \gamma_{i,k}\tilde{q}_k\} \end{aligned} \tag{A1}$$

and some properties of the gamma matrices:

$$\begin{aligned} &\sum_{i=1}^{N} \gamma_{i,k}^4 = \frac{3}{2}\frac{1}{N\chi^2}, \qquad &&\sum_{i=1}^{N} \gamma_{i,j}^2 \gamma_{i,k}^2 = \frac{1}{N\chi^2} \\ &\sum_{i=1}^{N} \gamma_{i,j}\gamma_{i,l}\gamma_{i,k}^2 = \frac{1}{2N\chi^2} \Delta(jlk), \qquad &&\sum_{i=1}^{N} \gamma_{i,j}\gamma_{i,k}^3 = \frac{1}{N\chi^2} \Delta(jk) \end{aligned} \tag{A2}$$

Different indices, i.e., $\{j, l, k\}$, do not assume simultaneously the same values, and the functions Δ are simple combinations of few ordinary Kronecker δ. The properties (A2) derive from trivial trigonometric properties.

The term in $\tilde{q}_k^4$ in (A1) is easily evaluated through (A2):

$$\left\langle \sum_{i=1}^{N} \gamma_{i,k}^4 \tilde{q}_k^4 \right\rangle_T = \frac{3}{N\chi^2} \langle \tilde{q}_k^4 \rangle_T \tag{A3}$$

which vanishes for growing N. As for the term in $\tilde{q}_k^2$, from (13) and (A2),

$$\begin{aligned}
&\left\langle \sum_{i=1}^{N} \{[(x_i - x_{i+1}) - \gamma_{i,k}\tilde{q}_k]^2 \gamma_{i,k}^2 \tilde{q}_k^2\} \right\rangle_T \\
&\quad = \left\langle \sum_{i=1}^{N} \left[\left(\sum_{j=2(k)}^{N} \gamma_{i,j}\tilde{q}_j \right)^2 \gamma_{i,k}^2 \tilde{q}_k^2 \right] \right\rangle_T \\
&\quad = \left\langle \sum_{i=1}^{N} \left(\sum_{j=2(k)}^{N} \gamma_{i,j}^2 \tilde{q}_j^2 \gamma_{i,k}^2 \tilde{q}_k^2 \right) \right\rangle_T \\
&\qquad + 2 \left\langle \sum_{i=1}^{N} \left(\sum_{j=2(k)}^{N} \sum_{l=2(jk)}^{N} \gamma_{i,j}\gamma_{i,l}\tilde{q}_j\tilde{q}_l\gamma_{i,k}^2\tilde{q}_k^2 \right) \right\rangle_T \\
&\quad \approx \frac{1}{N\chi^2} \left\langle \sum_{j=2(k)}^{N} \tilde{q}_j^2 \tilde{q}_k^2 \right\rangle_T \approx \frac{1}{N\chi} \langle 2V_2 \rangle_T \langle \tilde{q}_k^2 \rangle_T
\end{aligned} \tag{A4}$$

The symbol $\sum_{j=2(k)}^{N}$ means the "incomplete" sum where the index j excludes the value k. Here all the contribution comes from the term with $\langle \tilde{q}_j^2 \tilde{q}_k^2 \rangle_T$, by substituting the whole sum for the incomplete one, and from the natural hypothesis that V_2 and $\tilde{q}_k^2$ are weakly correlated at large N, so that the time averages can be factorized. The second term is much smaller because of the cancellations in the time averages $\langle \tilde{q}_j \tilde{q}_l \tilde{q}_k^2 \rangle_T$ with different $\{j, l, k\}$. In fact, the $\tilde{q}_j$ are weakly coupled to each other and they have zero time average. Actually, there are two sums over j and l, but only one survives because of the $\Delta(jlk)$ introduced in (A2).

Similar arguments lead to the conclusion that also the term in $\tilde{q}_k^3$ in (A1) is negligible with respect to the previous one.

As for the last term,

$$\begin{aligned}
&\left\langle \sum_{i=1}^{N} \left[\left(\sum_{j=2}^{N} \gamma_{i,j}\tilde{q}_j - \gamma_{i,k}\tilde{q}_k \right)^3 \gamma_{i,k}\tilde{q}_k \right] \right\rangle_T \\
&\quad = \left\langle \sum_{i=1}^{N} \left[\left(\sum_{j=2}^{N} \gamma_{i,j}\tilde{q}_j - \gamma_{i,k}\tilde{q}_k \right)^2 \left(\sum_{j=2}^{N} \gamma_{i,j}\tilde{q}_j \right) \gamma_{i,k}\tilde{q}_k \right] \right\rangle_T \\
&\qquad - \left\langle \sum_{i=1}^{N} \left[\left(\sum_{j=2}^{N} \gamma_{i,j}\tilde{q}_j - \gamma_{i,k}\tilde{q}_k \right)^2 \gamma_{i,k}^2 \tilde{q}_k^2 \right] \right\rangle_T \equiv \mathbf{X}_k - \mathbf{Y}_k
\end{aligned} \tag{A5}$$

these last symbols being introduced for convenience. Indeed, the following slightly modified combination of $\mathbf{X}_k$ and $\mathbf{Y}_k$ holds:

$$\begin{aligned} 2\mathbf{X}_k - \mathbf{Y}_k &= 2\left\langle \sum_{i=1}^{N} \left[\left(\sum_{j=2}^{N} \gamma_{i,j}\tilde{q}_j - \gamma_{i,k}\tilde{q}_k \right)^2 \left(\sum_{j=2}^{N} \gamma_{i,j}\tilde{q}_j \right) \gamma_{i,k}\tilde{q}_k \right] \right\rangle_T \\ &\quad - \left\langle \sum_{i=1}^{N} \left[\left(\sum_{j=2}^{N} \gamma_{i,j}\tilde{q}_j - \gamma_{i,k}\tilde{q}_k \right)^2 \gamma_{i,k}^2 \tilde{q}_k^2 \right] \right\rangle_T \\ &= -\left\langle \sum_{i=1}^{N} \left[\left(\sum_{j=2}^{N} \gamma_{i,j}\tilde{q}_j - \gamma_{i,k}\tilde{q}_k \right)^2 \left(\sum_{j=2}^{N} \gamma_{i,j}\tilde{q}_j - \gamma_{i,k}\tilde{q}_k \right) \right] \right\rangle_T \\ &\quad + \left\langle \sum_{i=1}^{N} \left[\left(\sum_{j=2}^{N} \gamma_{i,j}\tilde{q}_j - \gamma_{i,k}\tilde{q}_k \right)^2 \left(\sum_{j=2}^{N} \gamma_{i,j}\tilde{q}_j \right)^2 \right] \right\rangle_T \end{aligned} \tag{A6}$$

Formulas (A5) and (A6) require different estimates above and below threshold. In the stochastic domain, at large N, the last two terms in (A6) are approximately equal to each other and (apart from the factor $\varepsilon/4$) to the anharmonic potential (10). In fact, they differ not for classes of contributions (e.g., all the squared terms, all the forth powers,...), but only for terms containing powers of the single $\tilde{q}_k$, which are a small fraction of the total. Therefore, we may conclude that

$$2\mathbf{X}_k - \mathbf{Y}_k \approx 0$$

and the approximation improves growing with N. From this, (A5), and (A4), we finally obtain

$$\begin{aligned} &\left\langle \sum_{i=1}^{N} \{[(x_i - x_{i+1}) - \gamma_{i,k}\tilde{q}_k]^3 \gamma_{i,k}\tilde{q}_k\} \right\rangle_T \\ &\quad \approx -\frac{1}{2}\mathbf{Y}_k \\ &\quad = -\frac{1}{2}\left\langle \sum_{i=1}^{N} \{[(x_i - x_{i+1}) - \gamma_{i,k}\tilde{q}_k]^2 \gamma_{i,k}^2 \tilde{q}_k^2\} \right\rangle_T \\ &\quad \approx -\frac{1}{\chi}\left\langle \frac{V_2}{N} \right\rangle_T \langle \tilde{q}_k^2 \rangle_T \end{aligned} \tag{A7}$$

By collecting (A1), (A4), and (A7), we obtain the ansatz (20) with the value $A = 2.5$, to be compared with the experimental value $A \approx 2.4$ given in (22). Also the partial estimates (A4) and (A7) have been numerically checked to be satisfied within the same few percent of confidence.

An analogous procedure gives the estimate (24) on the anharmonic potential V_4.

Below threshold, from (A5) it follows that $\mathbf{X}_k \approx \mathbf{Y}_k$: in fact, the only contributions come from products of $\tilde{q}_j$ and $\tilde{q}_k$ with $j \neq k$, which, in this domain, are nearly completely uncorrelated. On the contrary, the last two terms in (A6) cannot be considered equal to each other as before, since they depend on k via the initial conditions. Therefore, below threshold (A4) gives the whole estimate of α in (20), with $A = 3$, to be compared with the experimental value $A \approx 2.9$ given after (22).

REFERENCES

1. E. Fermi, J. Pasta, and S. Ulam, In *Collected Papers of E. Fermi*, Vol. 2 (University of Chicago, Chicago, 1965), p. 78.
2. F. Izrailev and B. V. Chirikov, *Sov. Phys. Dokl.* **11**:30 (1966); P. Bocchieri, A. Scotti, B. Bearzi, and A. Loinger, *Phys. Rev. A* **2**:2013 (1970); B. V. Chirikov, *Phys. Rep.* **52**:263 (1979); R. Livi, M. Pettini, S. Ruffo, M. Sparparglione, and A. Vulpiani, *Phys. Rev.* **31A**:1039 (1985); H. Kantz, *Physica D* **39**:322 (1989).
3. C. Alabiso, M. Casartelli, and P. Marenzoni, *Phys. Lett.* **183A**:305 (1993).
4. M. Casartelli and S. Sello, *Nuovo Cimento* **97B**:183 (1987); M. Casartelli and S. Sello, *Phys. Lett.* **112A**:249 (1985); M. Casartelli and S. Sello, In *Advances in Nonlinear Dynamics and Stochastic Processes, II*, G. Paladin and A. Vulpiani, eds. (World Scientific, Singapore, 1987); C. Alabiso, M. Casartelli, and S. Sello, *J. Stat. Phys.* **54**:361 (1989); C. Alabiso, M. Casartelli, and A. Scotti, *Phys. Lett.* **147A**:292 (1990).
5. C. Alabiso and M. Casartelli, *Phys. Lett.* **173A**:37 (1993).
6. H. Kantz, R. Livi, and S. Ruffo, *J. Stat. Phys.* **76**:627 (1994).
7. S. Ruffo, Private communications.